REVISTA INTERDISCIPLINAR DE PESQUISA EM ENGENHARIA

CILAMCE 2016

XXXVII IBERIAN LATIN AMERICAN CONGRESS ON COMPUTATIONAL METHODS IN ENGINEERING
BRASÍLIA - DF - BRAZIL

Fluid Structure Interaction on AGARD 445.6 wing at Mach 0.9

Paulo Augusto Strobel Freitas Silva

Marcus Vinicius Girão de Morais

paulostrobel@gmail.com

mvmorais@unb.br

University of Brasilia - UnB
Campus Darcy Ribeiro, 70910-900, Brasilia, Distrito Federal, Brazil

Abstract. *In general, Solid-Fluid interaction problems are too complex to be solved analytically. Then, these problems are analysed by experiments or numerical solutions. Since experiments in flow Mach 0.9 is too expensive, numerical simulations seem to be the best tool to assess it. In this sense, this project the fluid-structure interaction (FSI) problem will be illustrated using the AGARD 445.6 wing, which its experiment has been widely studied. The main objective of the present study is to perform a validation on a FSI simulation of this wing at Mach 0.9 and study aeroelastic properties using ANSYS-CFX. Since FSI deform structure of the wing and the flow around it, this study involves mesh deformation and a large number of iterations.*

Keywords: *CFD, FSI, Flutter, Agard 445.6*

1 Introduction

The high velocity on aircraft lead to thin wings which are more likely to a mechanical failures. Consequently, a flutter study on airplane wings and turbomachinery blades is a critical issue to asses the reliability of the aircraft. In this phenomenon, aerodynamics forces acts on the structure deforming it. In this sense, flutter is a result of the Fluid-Structure Interaction (FSI) and is commonly associated with complex physics such as shock wave, boundary layer collapse and oscillations. In this sense, an accurate prediction of flutter is a challenging problem which requires a powerful software and computational resources.

Over the last years advances in computer technology and developments in numerical methods turned a FSI problem problems able to be simulated. As this issue deals with both fluid and solid, the governing equations have to be couple by efficient algorithms. Therefore, it requires the simultaneous application of Computational Fluid Dynamics (CFD) code so as to solve the aerodynamic forces and Computational Structural Dynamics (CSD) code to determine the solid deformation. Therefore, a fluid motion generates forces on structures, which deform due these forces and then the fluid movement is also affected by the structural displacement which results in new forces an this loop goes on. Traditionally, each of these computational code have been developed in different numerical technique. While most of CFD solvers are based on Finite Volume Method (FVM), CSD solvers uses a Finite Element Method (FEM). As the former uses a Eulerian or spatially fixed-coordinate system and the latter uses a lagragian or material fixed-coordinate system some approaches must be done so as to get the interaction between the two simulation modules. Therefore, an interfacing technique is one of the key factor since these two codes must communicate efficiently.

In general, there are two methods used to couple a FSI problem in the time: fully and loosely. In the former model, the structural response delays behind the fluid solution. In addition, this method is limited to first-order accuracy in time anyhow of the temporal precision of the solvers (Melville & Morton 1998). On other hand, fully coupled communicate simultaneously by exchanging the aerodynamic loads and structural displacement within each interaction. Consequently, it also brings a computational difficulties such as instability during the solution process (Kamakoti & Shyy 2004).

In this work, a FSI problem will be present using the AGARD 445.6 which is a benchmark experiment Yates Jr (1987) of flutter phenomena. Then a extensive research have been done using this wing (Lee-Rausch & Batina 1993, 1996, Lesoinne & Farhat 1998, Liu et al. 2001, Geuzaine et al. 2003, Thirifay & Geuzaine 2008, Chen et al. 2007). More recently, (Goud et al. 2014) performed a simulation of FSI problem in this wing at Mach 0.9 and discussed the results concerning the pressure, turbulence kinetic energy and temperature over the wing. The objective of this paper is to perform a validation of flutter in Agard 445.6 wing at 0.9 mach using a commercial platform *Ansys* in a personal computer (*intel i-7 1.8GHZ - 16Gb RAM*).

2 AGARD 445.6 WING

The AGARD 445.6 wing was tested by Yates Jr (1987) in both air and Freon-12 in the 16 x 16 foot NASA Langley Research Center. The first numerical digit named in the wing is associated with the aspect ratio. then, the following two digits refer to the quarter-chord sweep angle ($45°$) and the last digit indicates the taper ratio (0,66). As it is shown in This wing was based in the Naca 65A004 airfoil with no twist or curvature along its length. The root chord of this model was 0,55m and the semi-span was 0,76m. The semi-span model was attached directly to the wind tunnel wall, therefore, the wing root is into the wall boundary layer. The test model used in the experiments (**?**) was constructed using laminated mahogany, which has different material properties in each direction. Also, the model used in tests was weakened by drilled hole

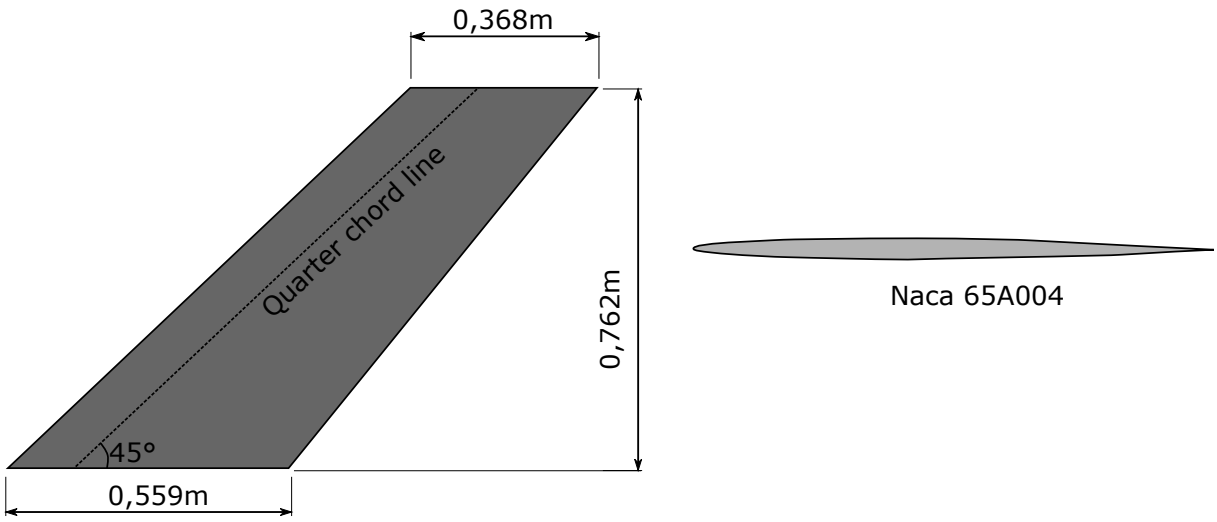

Figure 1: Wing Agard 445.6

The test model used in the experiments(Yates Jr 1987) was constructed by laminated mahogany, which has different material properties in each direction. Also, the model used in tests was weakened by drilled holes which were filled by foam in order to obtain easily the flutter conditions. The material properties in each direction for this weakened AGARD 445.6 wing is given in table x, where E id the Elasticity Modulus, G is Shear modulus and ρ is density.

Table 1: Material Properties for weakened AGARD 445.6 wing Yates Jr (1987)

Material Property	Valor
E_{11}	3.1511GPa
E_{22}	0.41621GPa
E_{33}	0.41621GPa
ν_{12}	0.31
ν_{13}	0.31
ν_{23}	0.31
G_{12}	0.4392 GPa
G_{23}	0.4392 GPa
G_{13}	0.4392 GPa
ρ	397 kg/m^3

3 Computational Structure Dynamics Modelling

In order to represent the deformation problem, the governing equations related to a structural dynamics is given by a stress strain relationship for a linear material as follows:

$$\overline{\sigma} = D\vec{\epsilon} \tag{1}$$

where $\overline{\sigma}$ is the stress tensor, D is the elasticity matrix and $\vec{\epsilon}$ is the train vector. Since *Ansys workbench* environment has a multi-physics platform, it provides a much easier for a user perform a fluid structure interaction. In this sense, so as to facilitate the communication between CFD and CSD, the Ansys transient structural solver was employed to deal with the solid governing equations.

The simulation process on Ansys passes through many steps from the geometry preparation to the solution. First, the Agard 445.6 wing was built by a CAD software, such as *Solidworks*, and imported into *Ansys*. In the next step, the mesh was generated in the wing, which reached a 11727 nodes. Then, the material properties of the mahogany were set according to data presented by Yates Jr (1987), which also is exposed in table 1. Last but not least, the boundary conditions were applied as shown in figure 2. Besides the gravitational forces in the y axis, the root wing was considered as fixed and in others wing surfaces, such as top,tip and bottom, were applied fluid structure interface. Also, the solver was set to perform a one sub-step per time-step, which is controlled defined by the CFD solver.

A similar procedure was done in the modal simulation. The main difference from the transient structural solver was the boundary conditions. In the modal part the wing root surface still fixed, however, the fluid-structure interfaces were not taking into account. In this matter, this solver were decoupled from the CFD part.

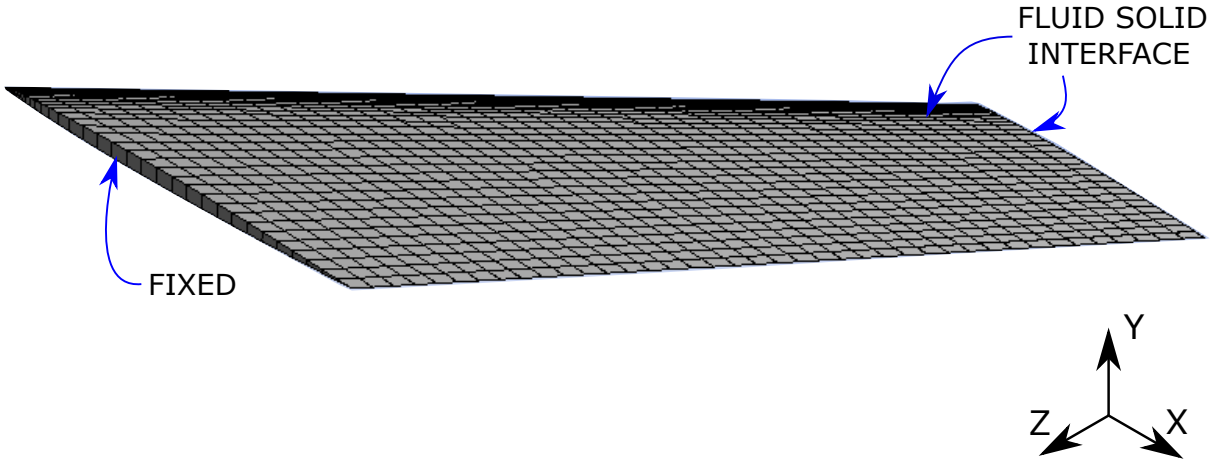

Figure 2: Solid mesh and boundary conditions of Wing Agard 445.6

4 Computational Fuid Dynamics Modelling

The fluid flow is assumed as compressible and fully turbulent. Consequently, velocity and pressure fields are governed by the Navier-Stokes equations. Due to the computational resource available, the turbulence phenomena was considered without numerically solving all the eddy scales. Then, the Unsteady Reynolds Averaged Navier-Stokes (URANS) approach was adopted. Hence, the governing equations of the flow are the continuity, momentum and energy conservation equations that can be described, respectively, as

$$\frac{\partial \rho}{\partial t} + \frac{\partial u_i}{\partial x_i} = 0 \tag{2}$$

$$\frac{\partial \rho u_i}{\partial t} + \frac{\partial \rho u_j u_i}{\partial x_j} = -\frac{\partial p}{\partial x_i} + \frac{\partial}{\partial x_i}(2\mu S_{ij} - \rho u_i u_j) + p f_i \tag{3}$$

$$\frac{\partial}{\partial t}\left[\rho\left(e + \frac{1}{2}u_i u_i\right)\right] + \frac{\partial}{\partial xj}\left[\rho u_j\left(h + \frac{1}{2}u_i u_i\right)\right] = \frac{\partial}{\partial x_j}[u_j(2\mu S_{ij} - \rho u_i u_j)] - \frac{\partial q_j}{\partial x_j} \tag{4}$$

where u_i are the components of the velocity, ρ is the density, p is the mechanical pressure, μ is the viscosity, f_j is a force per unit of volume such as gravitational force, e is specific internal energy, $h = e + p/\rho$ is specific enthalpy, and q_j is the heat flux vector. In the present work, the so-called $\kappa - \omega$ Shear-Stress Transport (SST) model, in the form as described by Menter (1993, 1994) Traditionally, in Reynolds Averaged Navier-Stokes (RANS) calculations, the steady-state solution is main objective. However, as the time interval used for the time averaging is reduces, and the transport equations are solved as dependent on time, an URANS scheme can be obtained.

The simulation were carried out by *Ansys CFX*, which is based on finite-volume method with an unstructured parallelized coupled algebric multigrid solver with a second order advection scheme. Moreover, the unsteady terms in the governing equations are solved by an implicit second order backward time-stepping algorithm.

The computational domain has a shape and dimensions as depicted in figure 3. The domain were assumed as big enough to represent the physics of the problem. The mesh generated for this domain achieved 505364 nodes. Then, the boundary conditions were applied in this domain in order to accurately represent the experiment as follows:

- Inlet velocity: a Dirichlet condition which is applied on the curved surface set a uniform velocity of $269,69ms^{-}1$ in the x direction with turbulence intensity of 5% and temperature of $269,86°K$. In this manner, the pressure is determined in a way to satisfy transport equations.
- Outlet pressure: in the upwind face another Dirichlet boundary condition was applied so as to define the pressure gauge as 0 Pa. Therefore, the velocity field is evaluated in order to satisfy transport equations.
- wall: a non-slip condition were applied to the wing surfaces, implying that the relative velocity of the fluid particle to the mesh motion is zero. Also, these surfaces wee set to has a interface with the CSD solver being able to receive data concerning the mesh displacement.
- Symmetry: applied on the lateral surface. In this condition, zero normal velocity at symmetry plane.
- Time-step: on the unsteady simulation was set a timestep of $0.0025s$ and a total time of $0.5s$.

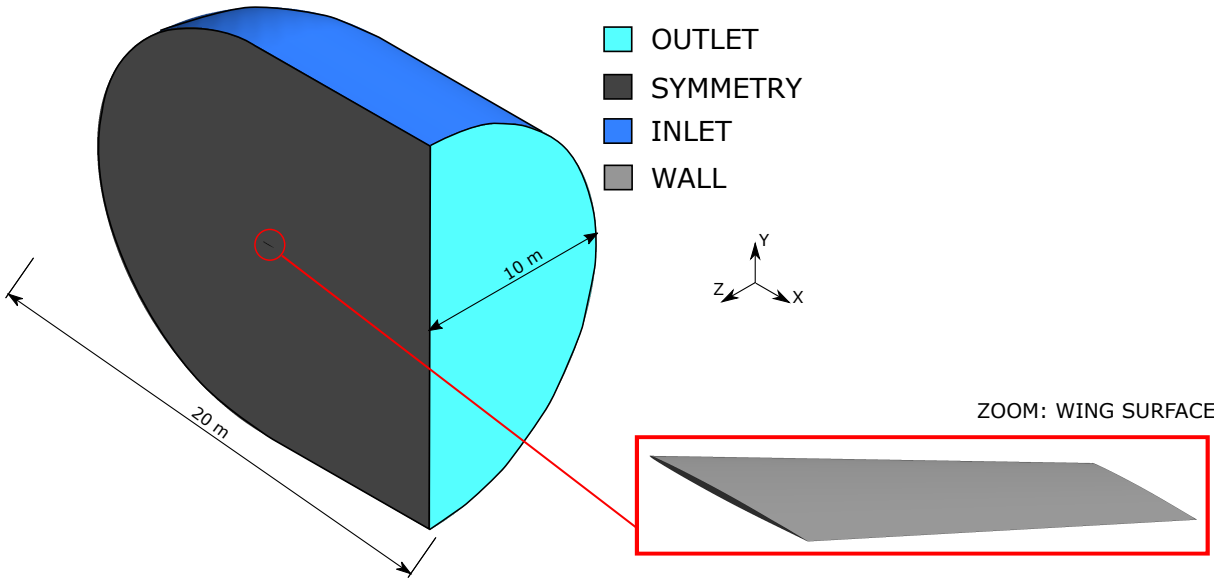

Figure 3: Computational CFD domain and boundary conditions

5 Overview of the Coupling

Ansys workbench software performs FSI by connecting the coupling participants to a component system named as System Coupling in a loosely-coupled method. In this sense, the participant, CSD and CFD, either feed or receives data into the coupled analysis. Firstly, the system collects information from the participants so as to adjust the system to start the simulation and then the information to be exchanged are given to the respective participant. Afterwards, the work process is organizing the sequence of transfer of information. Lastly, the convergence of coupling step is evaluated at end of every coupling iteration. In this case, as any time-step stars, CFD solver obtain the convergence in its own criteria and transfers the fluid forces to CSD solver. Hence, the displacement result of a CSD is solved using the solution provided by CFD for the same time-steps, as it is shown in figure 4 and 5.

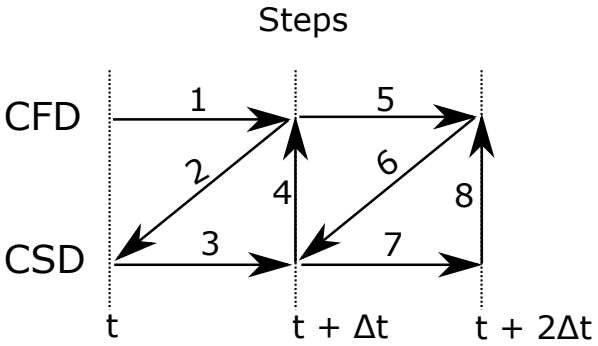

Figure 4: System coupling steps

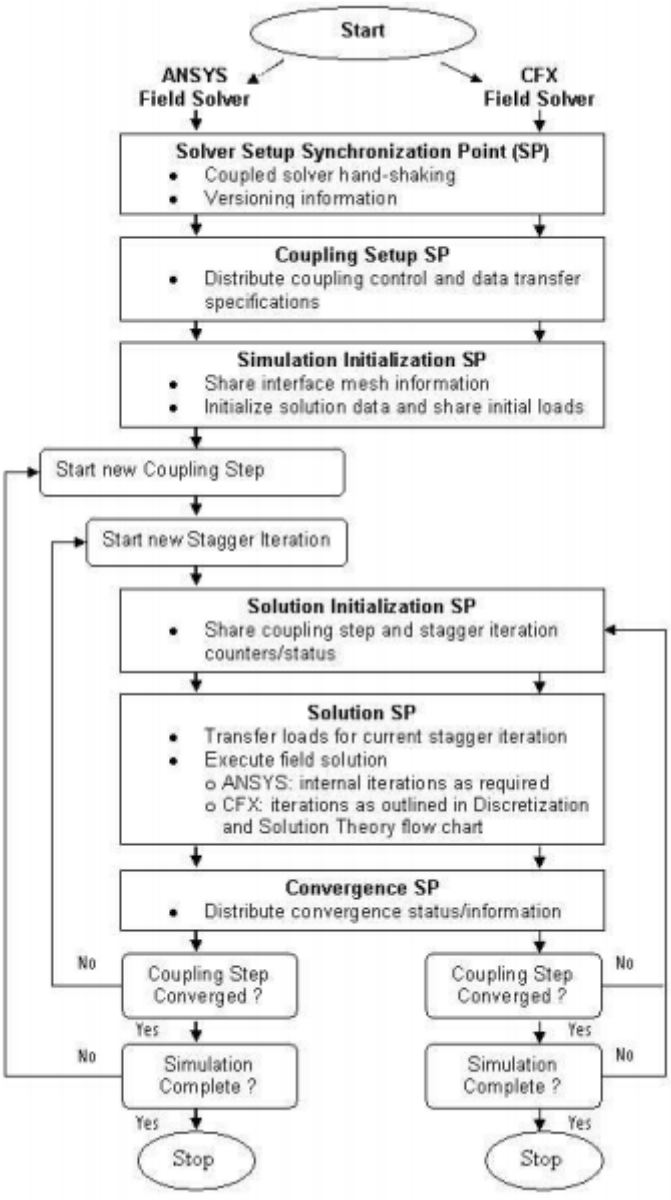

Figure 5: Problem Solution Procedure Ansys (2011)

At each time step showed in figure 4, four phase are done as follows:

A Solving the flow field as the boundary conditions are applied originally, shown in step 1

B Transferring data from CFD to CSD and converting the surface pressure to the general aerodynamic forces imposed in structural motion equations as showed in step 2.

C Performing structural motion equations, and updating the generalized displacement and velocity vector as showed in the step 3.

D Transferring data from CSD to CFD, and the aerodynamic mesh on the wing boundary is deformed in agreement with the structural distortion, shown in step 4.

E Solving the Navier Stokes equations again with the new boundary conditions and updating the variables of the flow field, shown in step 5.

Hence, by doing these steps successively, the time history resolution of both fluid and structure field are acquired.

6 Results and Discussion

6.1 Modal Validation

The modal data for the Agard 445.6 wing, in the form of the frequencies of the many natural nodes and its mode shapes were provided by Yates Jr (1987). Then, the numerical results of the first four frequencies were compared with the experimental data and other works as it is shown in table 2. It is noted that the results achieved here are well agreed with the experiment of Yates Jr (1987). In addition, as shown in figure 6 the contour of the mode frequencies also are similar to the experiment.

Table 2: Frequency comparison

	Present work	Ayabakan (2008)	Experiment (Yates Jr 1987)	Zuijlen (2007)
First mode [Hz]	9.6185	9.60	9.60	9.59
Second mode [Hz]	40.104	40.47	38.10	40.23
Third mode [Hz]	50.41	50.92	50.7	50.69
Fourth mode [Hz]	96.664	98.11	98.5	97.52

6.2 Flutter analysis

Before the flutter analysis of the wing takes place, the steady state response of the wing was numerically solved with the freestream conditions set to $u_x = 269.69$ m/s, $u_y = 0.26969$ m/s and $T = 269.86°K$. A steady state solution was first computed to a undeformed wing. Then, this perturbation fo the steady state solution was used as an initial condition for the unsteady state. In this part, u_y was set equal to zero and u_x remained at the same value. As mentioned before, it was set a time step $\Delta t = 0.0025s$ and a total time of $0.5s$ and the displacement of both tip leading and trailing edge was monitored in time as show in figure 8. As it is clearly noted there are a damping in the displacement over the time. In addition, it is noted that even though the velocity far away from the wing is set in 0.8 Mach, at the leading edge it reaches 0.9 Mach as can be seen in figure 7. In this sense, for the flutter analysis on the leading edge, the velocity at 0.9 Mach was considered to compare against experimental results.

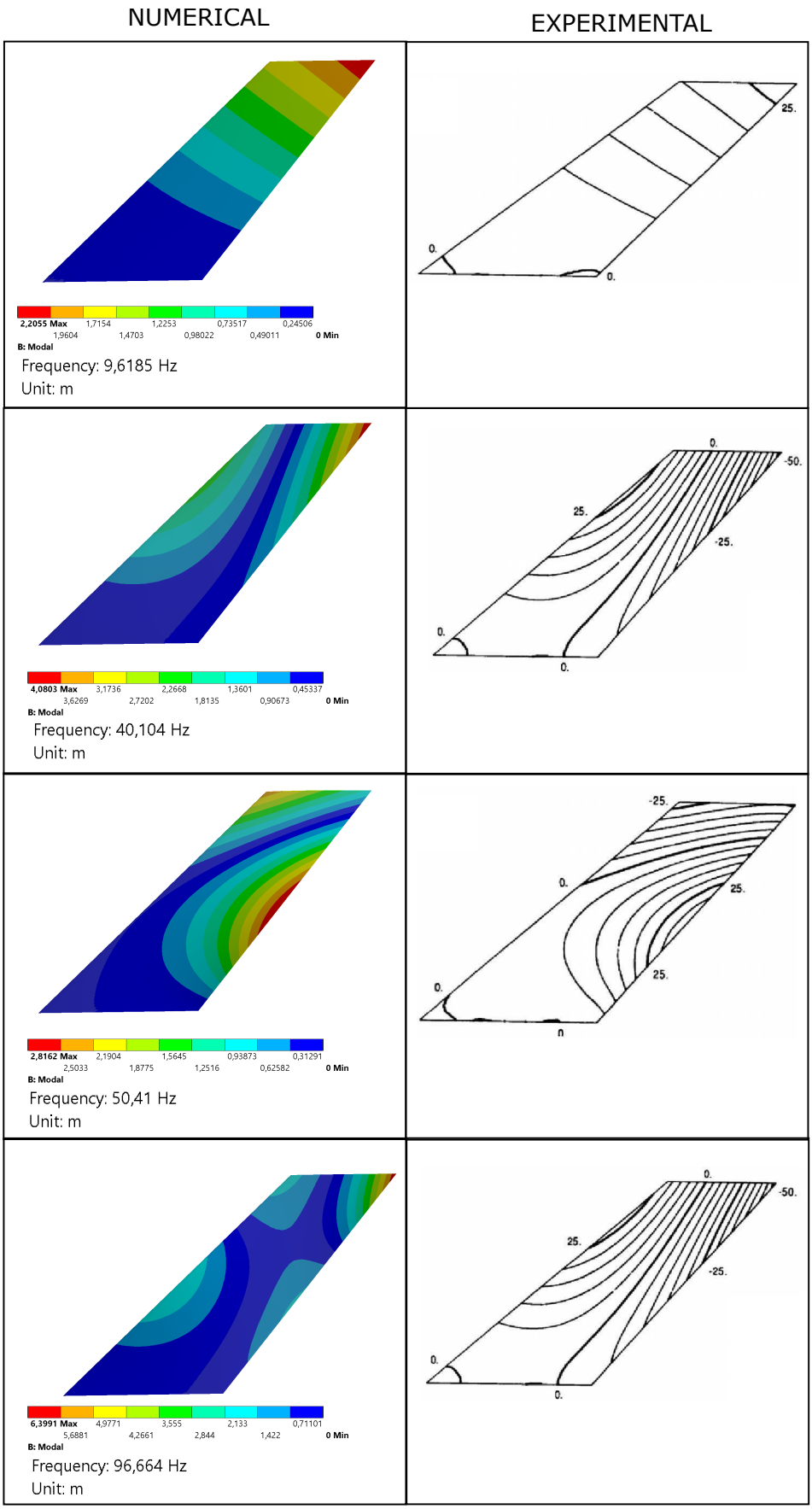

Figure 6: Mode shape comparison of the four modes

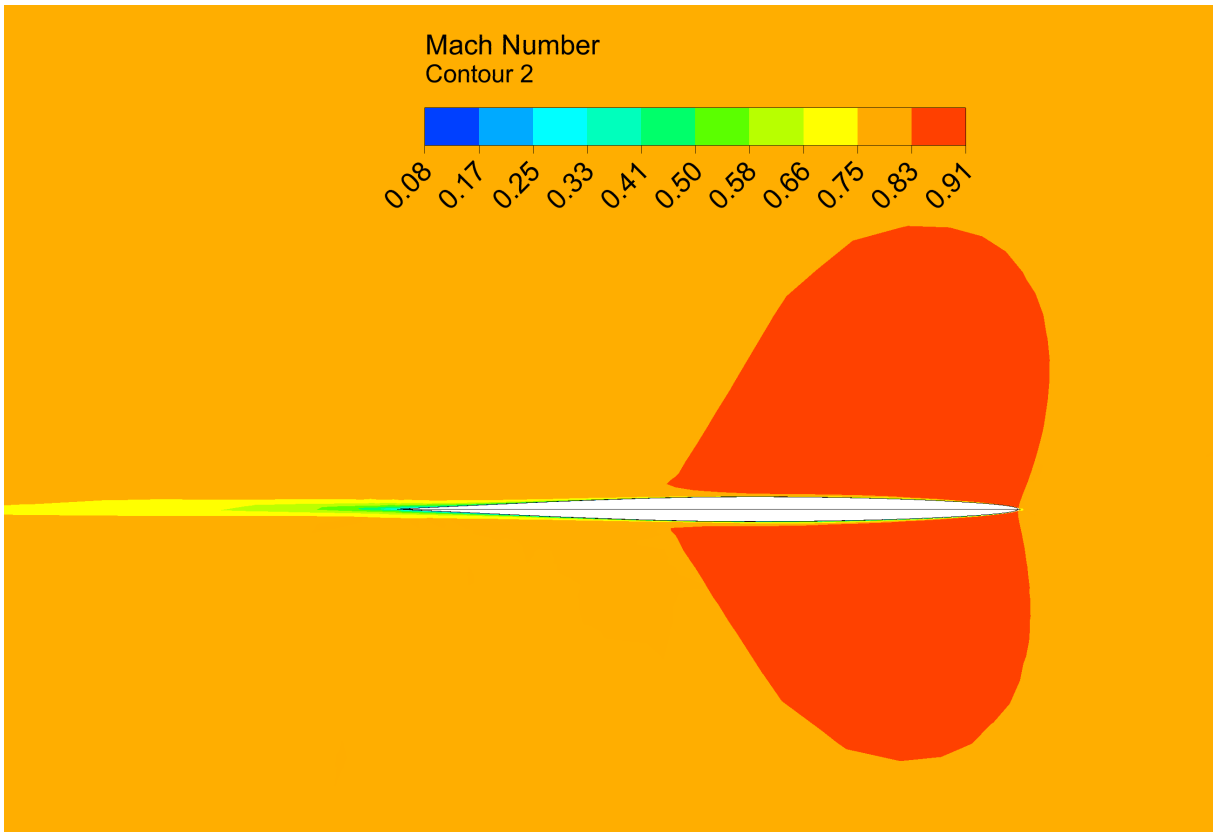

Figure 7: Mach number at the leading and trailing edge

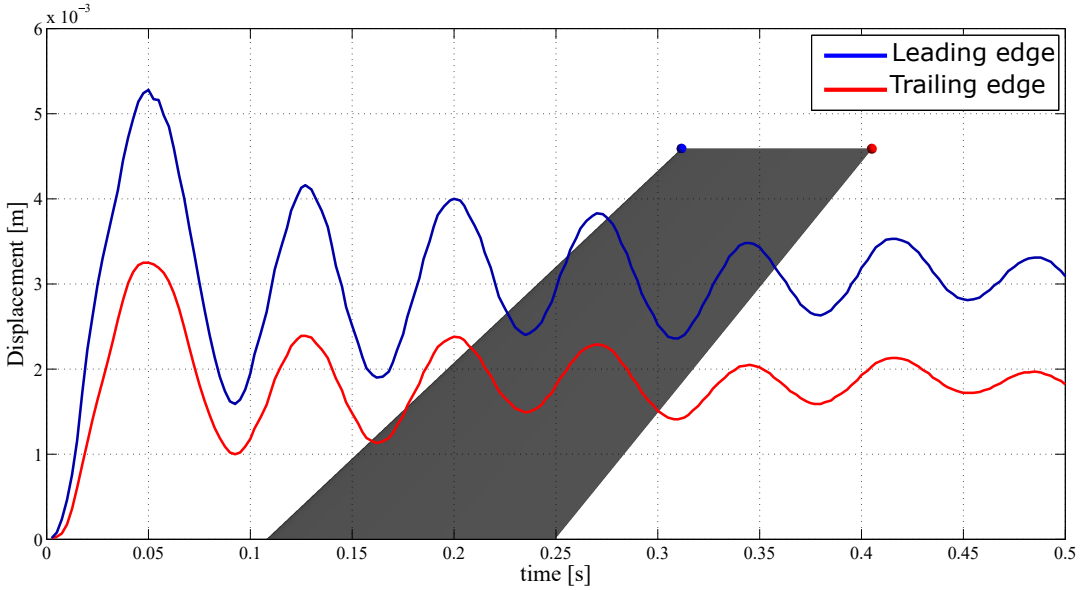

Figure 8: Tip and Leading edge mesh displacement.

So as to obtain the flutter frequency, a Fast Fourier Transform (FFT) is applied on the tip leading edge displacement data as shown in figure 9. The small bump around $7Hz$ is associated to data corruption that may be occurred due to the initial perturbation in the system. Hence, the first peak at $14Hz$ is the flutter frequency concerning the first bending mode ($9.6Hz$). Also, the small bump around $50Hz$ is likely to be the first torsion mode ($38.10Hz$), which requires smaller timesteps to be solved accurately. Thereby, to reach further modal modes

it is required a finer mesh and smaller timesteps. In this sense, as the experimental flutter frequency is $20.3Hz$ (Yates Jr 1987), the numerical result achieved here presents an error of 31%.

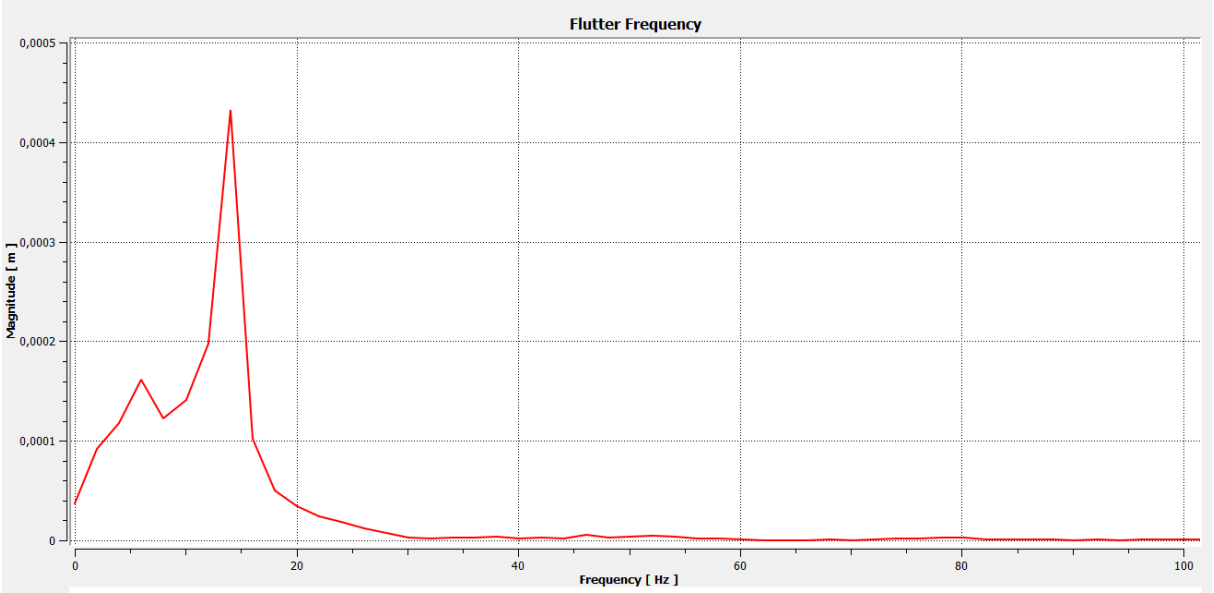

Figure 9: Flutter Frequency.

7 Conclusions

This work was largely aimed at giving a basic understanding and an overview of the fundamental FSI problem using a benchmark experiment such as AGARD 445.6 wing and complex phenomena like mesh motion and compressible flow in a personal computational resource. As previously mentioned, FSI plays a crucial role in many engineering fields which in many cases neglected due to lack of resources. In this sense, the present study performed a classic FSI flutter problem by a *intel i-7 1.8GHZ - 16Gb RAM* computer using a commercial software, which ran for 23 hours using only one core. It is important to mention that concepts and results achieved in studies like this one can be easily used as educational practices, as the limitations of mesh used here fit in an student license provided by *Ansys*. In addition, a finer mesh and smaller time-step would provide a better accuracy of results, especially in flutter frequency. All in all, the content presented here provides a great exposure of Fluid Structure Interaction flutter problem of a wing at Mach 0.9.

ACKNOWLEDGEMENTS

The authors would like to thanks University of Brasilia - UnB and Laboratory of Energy and Environment for all support.

References

Ansys, A. F., 2011. '14.0 theory guide', *ANSYS inc* pp. 218–221.

Ayabakan, S., 2008. Loosely-coupled flutter analysis of agard wing 445.6, *in* MpCCi, ed., '*9th MpCCI User Forum*', pp. 53–61.

Chen, X., Zha, G.-C. & Yang, M.-T., 2007. 'Numerical simulation of 3-d wing flutter with fully coupled fluid–structural interaction', *Computers & fluids* pp. 36,5,856–867.

Geuzaine, P., Grandmont, C. & Farhat, C., 2003. 'Design and analysis of ale schemes with provable second-order time-accuracy for inviscid and viscous flow simulations', *Journal of Computational Physics* pp. 191,1,206–227.

Goud, T. S. K., Sai Kumar, A. & Prasad, S. S., 2014. 'Analysis of fluid-structure interaction on an aircraft wing', *Analysis* **3**(9).

Kamakoti, R. & Shyy, W., 2004. 'Fluid–structure interaction for aeroelastic applications', *Progress in Aerospace Sciences* pp. 40,8,535–558.

Lee-Rausch, E. & Batina, J. T., 1996. 'Wing flutter computations using an aerodynamic model based on the navier-stokes equations', *Journal of Aircraft* pp. 33,6,1139–1147.

Lee-Rausch, E. M. & Batina, J. T., 1993. 'Calculation of agard wing 445.6 flutter using navier-stokes aerodynamics', *AIAA paper* pp. 3476,9–11.

Lesoinne, M. & Farhat, C., 1998. 'Higher-order subiteration-free staggered algorithm for nonlinear transient aeroelastic problems', *AIAA journal* pp. 36,9,1754–1757.

Liu, F., Cai, J., Zhu, Y., Tsai, H. & F. Wong, A., 2001. 'Calculation of wing flutter by a coupled fluid-structure method', *Journal of Aircraft* pp. 38,2,334–342.

Melville, R. B. & Morton, S., 1998. 'Fully-implicit aeroelasticity on overset grid systems', *AIAA Paper-98-0521* .

Menter, F. R., 1993. 'Zonal two equation k-turbulence models for aerodynamic flows', *AIAA paper* pp. 2906,1993.

Menter, F. R., 1994. 'Two-equation eddy-viscosity turbulence models for engineering applications', *AIAA journal* pp. 32,8,1598–1605.

Thirifay, F. & Geuzaine, P., 2008. 'c', *URL http://citeseerx. ist. psu. edu/viewdoc/summary* .

Yates Jr, E. C., 1987. 'Agard standard aeroelastic configurations for dynamic response. candidate configuration i.-wing 445.6'.

Zuijlen, A. V., 2007. High-order time integration throuh smooth mesh deformation for 3-d fluid-structure interation simulations, *in* MpCCi, ed., 'Journal of Computational Physics', pp. 224,414–4430.